Distortions in the Surface of Last Scattering

Peikai Li,[1] Scott Dodelson,[1] and Wayne Hu[2]

[1]*Department of Physics, Carnegie Mellon University, Pittsburgh, Pennsylvania 15312, USA*
[2]*Kavli Institute for Cosmological Physics, Department of Astronomy & Astrophysics,
Enrico Fermi Institute, The University of Chicago, Chicago, IL 60637, USA*

The surface of last scattering of the photons in the cosmic microwave background is **not** a spherical shell. Apart from its finite width, each photon experiences a different gravitational potential along its journey to us, leading to different travel times in different directions. Since all photons were released at the same cosmic time, the photons with longer travel times started farther away from us than those with shorter times. Thus, the surface of last scattering is corrugated, a deformed spherical shell. We present a quadratic estimator that could provide a map of the time delays as a function of position on the sky. The signal to noise of this map could exceed unity on large scales.

DISTANCE TO THE LAST SCATTERING SURFACE

The theory of general relativity dictates that particles traveling through gravitational potential wells experience time delays [?]. If two photons are emitted at the same time, then they will travel different distances depending upon the potential Φ through which they travel. In the cosmological context of an expanding, Euclidean universe what does Euclidean mean here? spatially flat background? , the fractional difference in comoving distance D_* to a source at redshift z_* is

$$d(\hat{n}) = \frac{2}{D_*} \int_0^{D_*} dD\, \Phi\left(D\hat{n}; t(D)\right) \qquad (1)$$

where $t(D)$ is the age of the universe when the photon is a comoving distance D from us, and we use the space-time metric convention

$$ds^2 = -(1 + 2\Phi)dt^2 + a^2(1 - 2\Phi)d\vec{x}^2 \qquad (2)$$

with $a(t)$ the scale factor. Note the sign in Eq. (1): if photons pass through an over-dense region where $\Phi < 0$, then they experience a time delay and therefore they arrive from a closer distance than the unperturbed last scattering surface[1].

Photons that comprise the cosmic microwave background (CMB) experience these same time delays or advances [?] where z_* is the redshift corresponding to the last scattering surface. Since photons do not decouple instantaneously from the electron-proton plasma, the surface of last scattering is often said to have a finite width, and a more accurate expression for the fractional difference in distance traveled is

$$d(\hat{n}) = 2 \int_0^{\infty} dz\, e^{-\tau(z)}\, K_d(z)\Phi\left(D(z)\hat{n}; t(z)\right) \qquad (3)$$

---

[1] There is also a geometric time delay that is typically of the same size for a single lens but is much smaller here on the large scales of interest.

where $H(z)$ is the Hubble expansion rate; $K_d(z) = (H(z)D_*)^{-1}$ and $D_* = \int_0^{\infty} dz' e^{-\tau(z')}/H(z')$. with τ being the optical depth, ignoring reionization, which becomes very large at times smaller than the epoch of last scattering, t_* or equivalently when $z > z_*$. This directional-dependent change in the distance to last scattering is independent of its finite width and is a phenomenon difference something not parsing here from the angular deflections [? ?] that have been captured by recent experiments [? ? ? ? ?].

Although deflections and delays are two different phenomena, they share some similarities, especially in the case of the CMB. Both are determined by the integrated potential along the line of sight, although with slightly different kernels, as depicted in Figure 1: the integrated potential ϕ that determines deflections has the same form as the right-hand side of Eq. (3) with

$$K_\phi(z) = \frac{D_* - D(z)}{D(z)D_*H(z)}. \qquad (4)$$

It is clear that they will be highly correlated, so as a first approximation, we might view the maps of the lensing potential created for example in ?] as maps of distance to the last scattering surface. Another similarity, one that has not yet been exploited, is that the quadratic estimator formalism [?] can be applied to the delays as well, and this is what we will do in this paper. We start though with the rather daunting facts that the RMS fractional distance differences are a factor of ten smaller than the RMS angular deviations and their impact on CMB power spectra is even smaller [?]. Further, while the latter peaks at degree scales, the former peak on the largest scales where cosmic variance is higher.

EFFECT OF DISTANCE CHANGES ON THE CMB

The observed temperature in a given direction $\Theta^{\text{obs}}(\hat{n})$ is the undistorted temperature $\tilde{\Theta}(\hat{n})$ plus the deflection
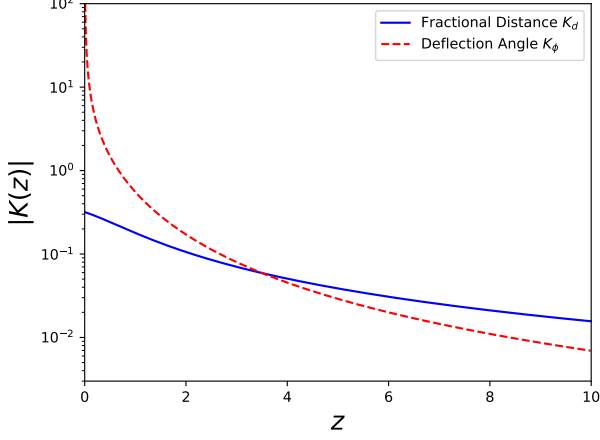
FIG. 1. Kernel that weights the integral of the gravitational potential for the time delay examined here and the more carefully studied deflection angle.

due to gravitational lensing plus a term proportional to the small fractional difference $d(\hat{n})$

$$\Theta^{\mathrm{obs}}(\hat{n}) = \tilde{\Theta}(\hat{n}) - \nabla_i \phi(\hat{n})\nabla^i \tilde{\Theta}(\hat{n}) - \frac{\partial \tilde{\Theta}(\hat{n})}{\partial \ln D_*}d(\hat{n}). \quad (5)$$

The third term's derivative can be evaluated by recalling that the undistorted temperature can be expanded in spherical harmonics with coefficients

$$\tilde{\Theta}_{lm} = 4\pi(-i)^l \int \frac{d^3k}{(2\pi)^3}Y^*_{lm}(\hat{k})S(\vec{k};\eta_*)j_l(kD_*), \quad (6)$$

where S is the source function, dominated on small scales by the monopole and dipole, as in Eq. (22) of Ref. [**?**]. The derivative with respect to distance then acts on the spherical Bessel function, and after expanding the fractional difference in spherical harmonics as well, we obtain

$$\Theta^{\mathrm{obs}}_{lm} = \tilde{\Theta}_{lm} - \delta\Theta^{\mathrm{defl}}_{lm} - \delta\Theta^{\mathrm{dist}}_{lm} \quad (7)$$

with the two first order terms due to deflection and the change in distance equal to

$$\delta\Theta^{\mathrm{defl}}_{lm} = \sum_{LM}\sum_{l'm'} {}_0I^{mMm'}_{lLl'}\tilde{\Theta}_{l'm'}\phi_{LM}, \quad (8)$$

$$\delta\Theta^{\mathrm{dist}}_{lm} = \sum_{LM}\sum_{l'm'} {}_0J^{mMm'}_{lLl'}\frac{\partial\tilde{\Theta}_{l'm'}(D_*)}{\partial \ln D_*}d_{LM}. \quad (9)$$

Here, we have written the integral over the product of three spherical harmonics as ${}_0I$ and ${}_0J$ to enable generalization to the case of polarization, which involves spin $s = 2$ harmonics. The general expression is

$${}_sI^{mMm'}_{lLl'} = (-1)^m \begin{pmatrix} l & L & l' \\ -m & M & m' \end{pmatrix}{}_sF_{lLl'}, \quad (10)$$

$${}_sJ^{mMm'}_{lLl'} = (-1)^m \begin{pmatrix} l & L & l' \\ -m & M & m' \end{pmatrix}{}_sG_{lLl'}, \quad (11)$$

with

$${}_sF_{lLl'} \equiv \left[L(L+1) - l'(l'+1) + l(l+1)\right]$$
$$\times \frac{\left[(2l+1)(2L+1)(2l'+1)\right]^{1/2}}{\sqrt{16\pi}}\begin{pmatrix} l & L & l' \\ s & 0 & -s \end{pmatrix},$$

$${}_sG_{lLl'} \equiv \frac{\left[(2l+1)(2L+1)(2l'+1)\right]^{1/2}}{\sqrt{4\pi}}\begin{pmatrix} l & L & l' \\ s & 0 & -s \end{pmatrix}. \quad (12)$$

Note the extra two powers of the multipoles in the function F that governs deflection; these follow from the fact that both the temperature and the potential are differentiated with respect to transverse position on the sky. By contrast, the radial derivative that governs the impact of the time delay, or change in distance to the last scattering surface, appears in Eq. (9) as the logarithmic derivative of the unlensed coefficients $\tilde{\Theta}_{LM}$.

As in the case of the effect of deflections on the CMB, the varying distances to the last scattering surface leads to correlations between l-modes that differ from one another. We proceed as in Ref. [**?**] by focusing on the expectation of off-diagonal $(l_1, m_1 \neq l_2, m_2)$ terms quadratic in the observed moments:

$$\langle\Theta^{\mathrm{obs}}_{l_1m_1}\Theta^{\mathrm{obs}}_{l_2m_2}\rangle = \sum_{LM}(-1)^M\begin{pmatrix} l_1 & l_2 & L \\ m_1 & m_2 & -M \end{pmatrix}$$
$$\times\left[\phi_{LM}f_{l_1Ll_2} + d_{LM}g_{l_1Ll_2}\right], \quad (13)$$

where

$$f_{l_1Ll_2} \equiv \left[\tilde{C}^{\Theta\Theta}_{l_1}{}_0F_{l_2Ll_1} + \tilde{C}^{\Theta\Theta}_{l_2}{}_0F_{l_1Ll_2}\right],$$
$$g_{l_1Ll_2} \equiv \left[\tilde{C}^{\Theta\Theta,d}_{l_1}{}_0G_{l_2Ll_1} + \tilde{C}^{\Theta\Theta,d}_{l_2}{}_0G_{l_1Ll_2}\right]. \quad (14)$$

The change in distance to the last scattering spectrum produces the spectrum

$$C^{\Theta\Theta,d}_l \equiv \frac{2}{\pi}\int_0^\infty dk\,k^2\,P_S(k,\eta_*)\,j_l(kD_*)\frac{\partial j_l(kD_*)}{\partial \ln D_*} \quad (15)$$

with P_S the power spectrum of the source. This expression is identical to the one for the undistorted CMB spectrum C_l other than the replacement $j_l \to j'_l$. The two spectra are shown in Fig. 2. We modify the public CAMB code and account for the finite thickness of the last scattering surface. More words on this? similar comment on the polarization analogues below.

Note the difference between these two functions. Each involves a derivative. The one that governs deflections, f, involves a derivative with respect to the transverse directions so F as defined in Eq. (12) has more powers of l than does G. The function that governs changes in distances involved a radial derivative, and this shows up in the spectrum $C^{\Theta\Theta,d}_l$.

The correlation between different l-modes enables us, following Ref. [**?**], to extract information about the fields causing these correlations by forming quadratic estimators for both the gravitational potential responsible for
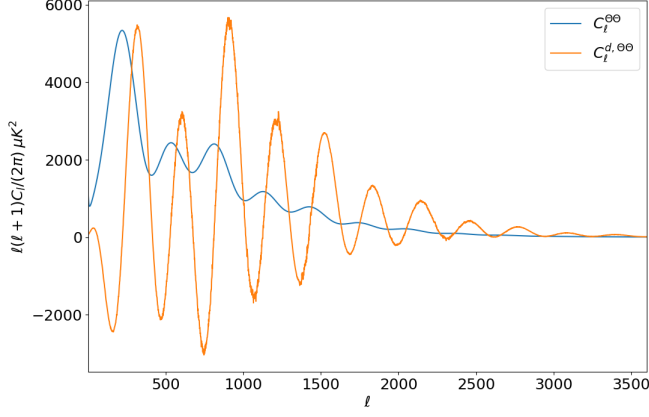
FIG. 2. Spectra of CMB temperature anisotropies and the logarithmic derivative of that spectrum with respect to the distance to the last scattering surface as defined in Eq. (15).

deflections and the fractional distance field:

$$\hat{\phi}_{LM} = A_L \sum_{l_1 m_1} \sum_{l_2 m_2}$$
$$(-1)^M \begin{pmatrix} l_1 & l_2 & L \\ m_1 & m_2 & -M \end{pmatrix} h^{\phi}_{l_1 l_2}(L) \Theta^{\mathrm{obs}}_{l_1 m_1} \Theta^{\mathrm{obs}}_{l_2 m_2} \quad (16)$$

$$\hat{d}_{LM} = B_L \sum_{l_1 m_1} \sum_{l_2 m_2}$$
$$(-1)^M \begin{pmatrix} l_1 & l_2 & L \\ m_1 & m_2 & -M \end{pmatrix} h^{d}_{l_1 l_2}(L) \Theta^{\mathrm{obs}}_{l_1 m_1} \Theta^{\mathrm{obs}}_{l_2 m_2} \quad (17)$$

where

$$h^{\phi}_{l_1 l_2}(L) \equiv \frac{f_{l_1 L l_2}}{2 C_{l_1} C_{l_2}} \quad (18)$$

$$h^{d}_{l_1 l_2}(L) \equiv \frac{g_{l_1 L l_2}}{2 C_{l_1} C_{l_2}} \quad (19)$$

and

$$A_L \equiv (2L+1) \left\{ \sum_{l_1 l_2} h^{\phi}_{l_1 l_2}(L) f_{l_1 L l_2} \right\}^{-1} \quad (20)$$

$$B_L \equiv (2L+1) \left\{ \sum_{l_1 l_2} h^{d}_{l_1 l_2}(L) g_{l_1 L l_2} \right\}^{-1}. \quad (21)$$

With these definitions, the expectation values of the two estimators are equal to ϕ_{LM} and d_{LM} respectively.

The noise on these estimators is now given by the prefactors A_L and B_L, so

$$\langle \hat{d}_{LM} \hat{d}^*_{L'M'} \rangle = \delta_{LL'} \delta_{MM'} \left(C^{dd}_L + B_L \right) \quad (22)$$

with the first term on the right the signal and the second the noise. Fig. 3 shows the signal and noise at each L for several experimental configurations. Since the signal can be extracted from all available d_{LM}, the total signal to noise for a measurement is

$$\left(\frac{S}{N} \right)^2 = \sum_{L}^{\infty} \frac{(2L+1) f_{\mathrm{sky}}}{2} \left(\frac{C^{dd}_L}{C^{dd}_L + B_L} \right)^2. \quad (23)$$

This doesn't look right to me at least the mode counting is inverted but I also don't understand what S/N this is - I suggest you define the signal to noise as the number of sigma that you an detect the given power spectrum as in my note. Also, the connection with what is plotted in the figure isn't made explicit here. We see that most of the signal arises from the lowest L-modes, particularly $L = 1$. However, even for a full-sky experiment, the most optimistic niose projections lead to a total signal to noise less than 1, using temperature only.
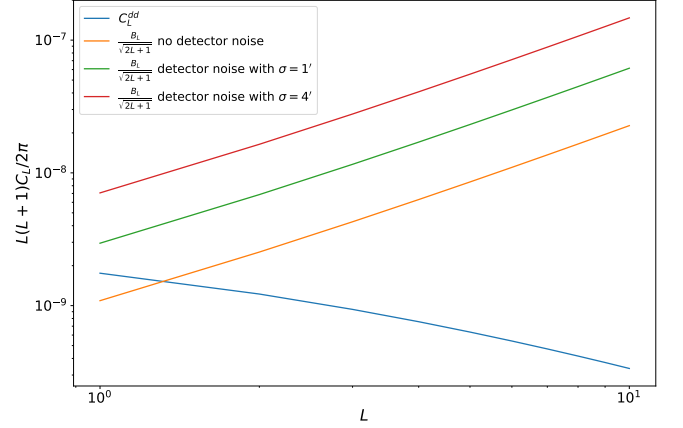

FIG. 3. Signal (decreasing blue curve) due to the distorted surface of last scattering and the noise using the quadratic estimator constructed from the small scale temperature anisotropy ($\Theta\Theta$ in the notation of Table 1) for several different experimental configurations. Most optimistic is no noise out to $l_{\max} = 7000$; the other two noise curves have sensitivity of 1μK-arcmin and beam size. $\theta_{\mathrm{FWHM}} = 1'$ or $4'$. Here, f_{sky} is set to one.

POLARIZATION

The estimator above used only the temperature anisotropy field, but the polarization field contains even more information about the lensing potential that governs deflection and distance changes. This was worked out in detail by Ref. [?] for deflection, and we follow their notation here. There are now three fields of interest: temperature Θ, and the two fields associated with polarization, E and B. With letters a, b each ranging over these three fields, we have

$$\langle a^{obs}_{l_1 m_1} b^{obs}_{l_2 m_2} \rangle = \sum_{LM} (-1)^M \begin{pmatrix} l_1 & l_2 & L \\ m_1 & m_2 & -M \end{pmatrix}$$
$$\times \left[\phi_{LM} f^{\alpha}_{l_1 L l_2} + d_{LM} g^{\alpha}_{l_1 L l_2} \right]. \quad (24)$$

The functions f^{α} and g^{α} are the generalizations of Eq. (14) to include polarization (Eq. (14) now corresponds to $\alpha = \Theta\Theta$). The full set of f^{α} was determined

by Ref. [**?**] and is reproduced in Table 1, which now includes the full set of g^α that govern the impact of changing radial distances. Note that $\tilde{C}_l$ corresponds to the spectra of the unlensed fields. I think we should change the $\tilde{C} \to C$ here, since they are not the spectra of the unlensed fields: they are the radial derivatives of the spectra, right? They are radial derivatives of the unlensed (i.e. before lensing) fields Also, propose to add the following few lines, replacing the sentence above that starts "Note that ..." **Note that the angular deflection coefficients f^α included the unlensed field because the transverse derivatives are captured by powers of ℓ. The radial derivatives must be computed directly, as in Eq. (15). For example,**

$$C_l^{\Theta E,d} \equiv \frac{2}{\pi} \int_0^\infty dk \, k^2 \, P^{\Theta E}(k,\eta_*) \, j_l(kD_*) \, \frac{\partial j_l(kD_*)}{\partial \ln D_*} \tag{25}$$

with $P^{\Theta E}(k,\eta_*)$ the 3D cross-power spectrum at the time of recombination of the temperature field and the E-mode of the polarization field. We still need to comment on the link to what is actually done, which is to include the time variation of the source fields

α	$f_{l_1 L l_2}^\alpha$	$g_{l_1 L l_2}^\alpha$
$\Theta\Theta$	$\tilde{C}_{l_1}^{\Theta\Theta} {}_0F_{l_2 L l_1} + \tilde{C}_{l_2}^{\Theta\Theta} {}_0F_{l_1 L l_2}$	$\tilde{C}_{l_1}^{\Theta\Theta,d} {}_0G_{l_2 L l_1} + \tilde{C}_{l_2}^{\Theta\Theta,d} {}_0G_{l_1 L l_2}$
ΘE	$\tilde{C}_{l_1}^{\Theta E} {}_2F_{l_2 L l_1} + \tilde{C}_{l_2}^{\Theta E} {}_0F_{l_1 L l_2}$	$\tilde{C}_{l_1}^{\Theta E,d} {}_2G_{l_2 L l_1} + \tilde{C}_{l_2}^{\Theta E,d} {}_0G_{l_1 L l_2}$
EE	$\tilde{C}_{l_1}^{EE} {}_2F_{l_2 L l_1} + \tilde{C}_{l_2}^{EE} {}_2F_{l_1 L l_2}$	$\tilde{C}_{l_1}^{EE,d} {}_2G_{l_2 L l_1} + \tilde{C}_{l_2}^{EE,d} {}_2G_{l_1 L l_2}$
ΘB	$i\tilde{C}_{l_1}^{\Theta E} {}_2F_{l_2 L l_1}$	$i\tilde{C}_{l_1}^{\Theta E,d} {}_2G_{l_2 L l_1}$
EB	$i\big[\tilde{C}_{l_1}^{EE} {}_2F_{l_2 L l_1} - \tilde{C}_{l_2}^{BB} {}_2F_{l_1 L l_2}\big]$	$i\big[\tilde{C}_{l_1}^{EE,d} {}_2G_{l_2 L l_1} - \tilde{C}_{l_2}^{BB,d} {}_2G_{l_1 L l_2}\big]$
BB	$\tilde{C}_{l_1}^{BB} {}_2F_{l_2 L l_1} + \tilde{C}_{l_2}^{BB} {}_2F_{l_1 L l_2}$	$\tilde{C}_{l_1}^{BB,d} {}_2G_{l_2 L l_1} + \tilde{C}_{l_2}^{BB,d} {}_2G_{l_1 L l_2}$

TABLE I. Explicit forms for f anb h of various polarizations. Notice that for TT, TE, EE and BB polarization these functions are "even"; for TB and EB polarization they are "odd" instead. "Even" and "Odd" indicate that the functions are non-zero only when $l_1 + l_2 + L$ are even or odd, respectively.

An estimator can now be constructed for each of the pairs of fields (except BB), so letting α denote pairs of fields (ab), we have

$$\hat{d}_{LM}^\alpha = (-1)^M B_L^\alpha \sum_{l_1 m_1} \sum_{l_2 m_2} \begin{pmatrix} l_1 & l_2 & L \\ m_1 & m_2 & -M \end{pmatrix} \times h_{l_1 l_2}^{\alpha,d}(L) a_{l_1 m_1}^{obs} b_{l_2 m_2}^{obs}, \tag{26}$$

where the coefficients are generalizations of Eq. (21) with g and h there acquiring superscripts α. The g^α are given in Table 1 and the minimizing weights are

$$h_{l_1 l_2}^{\alpha=(ab),d}(L) = \frac{C_{l_2}^{aa} C_{l_1}^{bb} g_{l_1 L l_2}^{\alpha*} - (-1)^{L+l_1+l_2} C_{l_1}^{ab} C_{l_2}^{ab} g_{l_2 L l_1}^{\alpha*}}{C_{l_1}^{aa} C_{l_2}^{aa} C_{l_1}^{bb} C_{l_2}^{bb} - (C_{l_1}^{ab} C_{l_2}^{ab})^2} \tag{27}$$

with

$$h_{l_1 l_2}^{\alpha=(aa),d}(L) = \frac{g_{l_1 L l_2}^{\alpha*}}{2 C_{l_1}^{aa} C_{l_2}^{aa}}. \tag{28}$$

Note that in the special case when $C_l^{ab} = 0$ (e.g., for ΘB or EB), this reduces to

$$h_{l_1 l_2}^{\alpha,d}(L) \to \frac{g_{l_1 L l_2}^{\alpha*}}{C_{l_1}^{aa} C_{l_2}^{bb}}. \tag{29}$$

The covariance of these quadratic estimators

$$\langle \hat{d}_{LM}^{\alpha*} d_{L'M'}^\beta \rangle \equiv \delta_{LL'} \delta_{MM'} \big[C_L^{dd} + N_L^{d,\alpha\beta} \big] \tag{30}$$

with Gaussian noise given by

$$N_L^{d,\alpha\beta} = \frac{B_L^{\alpha*} B_L^\beta}{2L+1} \sum_{l_1 l_2} \Big\{ h_{l_1 l_2}^{\alpha,d*}(L) \big[C_{l_1}^{ac} C_{l_2}^{bd} h_{l_1 l_2}^{\alpha,d}(L) + (-1)^{L+l_1+l_2} C_{l_1}^{ad} C_{l_2}^{bc} h_{l_2 l_1}^{\beta,d}(L) \big] \Big\} \tag{31}$$

with $\alpha = (ab)$, $\beta = (cd)$. For $\alpha = \beta$, Eq. (37) reduces to $N_L^{d,\alpha\alpha} = B_L^\alpha$. Armed with these expressions, we can form a minimum variance estimator

$$\hat{d}_{LM}^{\mathrm{mv}} = \sum_\alpha \omega^\alpha(L) \hat{d}_{LM}^\alpha \tag{32}$$

with weights and variance given by

$$\omega^\alpha(L) = N_L^{d,\mathrm{mv}} \sum_\beta (N_L^{d,-1})^{\alpha\beta} \tag{33}$$

$$N_L^{d,\mathrm{mv}} = \frac{1}{\sum_{\alpha\beta} (N_L^{d,-1})^{\alpha\beta}} \tag{34}$$

where $N_L^{d,-1}$ is the inverse matrix of time delay noise given by Eq. (27), with matrix indices given by polarizations.

We saw in Fig. 3 that small scale temperature maps only are not sufficient to detect this signal. To assess the added information contained in the polarization field, we show the signal to noise for the lowest L-mode as a function $l_{\max}$ for a noiseless experiment in Fig. 4.

Here we keep $l_{\min}$ fixed at 1000 for the CMB fields (we tested that our final results are insensitive to this choice) and let $l_{\max}$ vary. We can see that at $l_{\max} \approx 5000$, the minimum variance estimator signal to noise reaches 1, but of course this is for the most optimistic of configurations. Any comments on the differences between lensing and delay estimators especially on B modes?

CONCLUSIONS

The last scattering surface of the CMB is not purely spherical due to the different travel times experienced by photons as they traverse the inhomogeneous gravitational potential. In principle, these distortions in the distance to different directions is detectable, but we conclude here that the standard auto-correlation techniques will not be sufficient to enable detection in the near future. There is the possibility of cross-correlating a map of
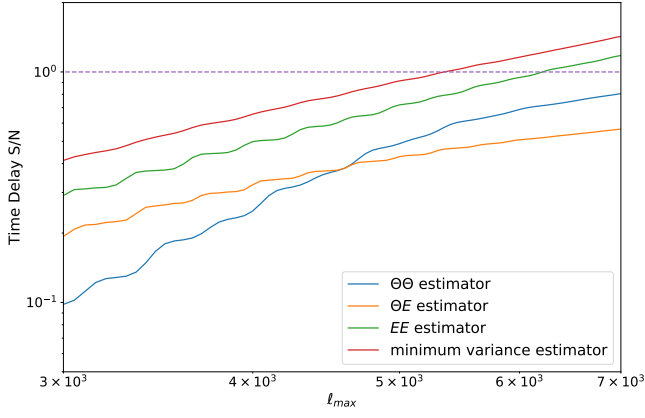
FIG. 4. Time Delay Signal to Noise, using Eq. (44) for different estimators. Here we set f_{sky} to be 1.

the distance distortions constructed with the quadratic estimators introduced here with another map of a closely related integrated potential and extracting the signal in that way. Indeed, this was the way that the transverse distortions in the CMB were first detected [?]. We have considered where the cross-correlation signal between the distance distortion and the standard transverse deviation maps can be detected and concluded that it cannot. We leave exploration of other cross-correlations for further work; however, we point out that yet another challenge confronted will be the fidelity of the distance distortion maps, as they are contaminated by the standard lensing signals.

Appendix A: Dectection of Cross Power Spectrum

With the existence of these two estimators, we can now construct a new estimator

$$\hat{C}_{LM}^{\phi d, \alpha\beta} = \hat{\phi}_{LM}^{\alpha*}\hat{d}_{LM}^{\beta} - \mathcal{N}_L^{\alpha\beta} \tag{35}$$

to estimate cross power spectrum, where $\mathcal{N}_L^{\alpha\beta}$ is the bias of the expectation value of $\hat{\phi}_{LM}^{\alpha*}\hat{d}_{LM}^{\beta}$ and the power spectrum

$$\langle \hat{\phi}_{LM}^{\alpha*}\hat{d}_{L'M'}^{\beta} \rangle = \delta_{LL'}\delta_{MM'}(C_L^{\phi d} + \mathcal{N}_L^{\alpha\beta}) \tag{36}$$

thus $\mathcal{N}_L^{\alpha\beta}$ is given similarly as $N_L^{\alpha\beta}$ by

$$\mathcal{N}_L^{\alpha\beta} = \frac{\bar{A}_L^{\alpha*}\bar{B}_L^{\beta}}{\sqrt{L(L+1)}(2L+1)}\sum_{l_1l_2}\left\{\bar{h}_{l_1l_2}^{\alpha,\phi*}(L)\left[C_{l_1}^{ac}C_{l_2}^{bd}\bar{h}_{l_1l_2}^{\alpha,d}(L) \right.\right.$$
$$\left.\left. + (-1)^{L+l_1+l_2}C_{l_1}^{ad}C_{l_2}^{bc}\bar{h}_{l_2l_1}^{\beta,d}(L)\right]\right\} \tag{37}$$

Notice that we can choose the definition of $\bar{h}$ to minimize covariance of $\hat{C}_{LM}^{\phi d,\alpha\beta}$, and the result is quite symmetric

$$\bar{h}_{l_1l_2}^{\alpha,\phi}(L) = h_{l_1l_2}^{\alpha,d}; \ \bar{h}_{l_1l_2}^{\alpha,d}(L) = h_{l_1l_2}^{\alpha,\phi}(L) \tag{38}$$

with

$$\bar{A}_L^\alpha = L(L+1)(2L+1)\left\{\sum_{l_1l_2}\bar{h}_{l_1l_2}^{\alpha,\phi}(L)f_{l_1Ll_2}^\alpha\right\}^{-1}$$

$$= L(L+1)(2L+1)\left\{\sum_{l_1l_2}h_{l_1l_2}^{\alpha,d}(L)f_{l_1Ll_2}^\alpha\right\}^{-1} \tag{39}$$

$$\bar{B}_L^\alpha = (2L+1)\left\{\sum_{l_1l_2}\bar{h}_{l_1l_2}^{\alpha,d}(L)g_{l_1Ll_2}^\alpha\right\}^{-1}$$

$$= (2L+1)\left\{\sum_{l_1l_2}h_{l_1l_2}^{\alpha,\phi}(L)g_{l_1Ll_2}^\alpha\right\}^{-1} \tag{40}$$

In this case

$$\mathcal{N}_L^{\alpha\alpha} = \bar{A}_L^\alpha/\sqrt{L(L+1)} = \bar{B}_L^\alpha\sqrt{L(L+1)}$$

$$= \sqrt{L(L+1)}(2L+1)\left\{\sum_{l_1l_2}h_{l_1l_2}^{\alpha,d}(L)f_{l_1Ll_2}^\alpha\right\}^{-1}$$

$$= \sqrt{L(L+1)}(2L+1)\left\{\sum_{l_1l_2}h_{l_1l_2}^{\alpha,\phi}(L)g_{l_1Ll_2}^\alpha\right\}^{-1} \tag{41}$$

One thing to notice that here the definition of A is the same as Okamoto & Hu. But it is easy to get the scale Scott suggested.

Finally the Gaussian covariance of $\hat{C}_{LM}^{\phi d,\alpha\beta}$ is

$$\langle \hat{C}_{LM}^{\phi d,\alpha\beta*}\hat{C}_{LM}^{\phi d,\gamma\sigma} - (C_L^{\phi d})^2\rangle/(2L+1)$$
$$= \left\{(C_L^{\phi d} + \mathcal{N}_L^{\alpha\beta})(C_L^{\phi d} + \mathcal{N}_L^{\gamma\sigma})\right.$$
$$+ (C_L^{\phi d} + \mathcal{N}_L^{\alpha\sigma})(C_L^{\phi d} + \mathcal{N}_L^{\beta\gamma})$$
$$+ (C_L^{\phi\phi} + N_L^{\phi,\alpha\gamma})(C_L^{dd} + N_L^{d,\beta\sigma})$$
$$- (C_L^{\phi d} + \mathcal{N}_L^{\alpha\beta})\mathcal{N}_L^{\gamma\sigma} - (C_L^{\phi d} + \mathcal{N}_L^{\gamma\sigma})\mathcal{N}_L^{\alpha\beta}$$
$$\left. + \mathcal{N}_L^{\alpha\beta}\mathcal{N}_L^{\gamma\sigma} - (C_L^{\phi d})^2\right\}/(2L+1) \tag{42}$$

When $(\alpha\beta) = (\gamma\sigma)$, this simplified to

$$\frac{1}{2L+1}\left\{(C_L^{\phi d} + \mathcal{N}_L^{\alpha\beta})^2 \right.$$
$$\left. + (C_L^{\phi\phi} + N_L^{\phi,\alpha\alpha})(C_L^{dd} + N_L^{d,\beta\beta})\right\} \tag{43}$$

And we can compute cross power spectrum signal-to-noise by assuming that $(C_L^{\phi d} + \mathcal{N}_L^{\alpha\beta}) = 0$ and use minimu variance estimator for both lensing and time delay. Signal-to-noise in FIG.5 is given by:

$$\left(\frac{S}{N}\right)^2 = \sum_L^\infty (2L+1)f_{\text{sky}}\frac{C_L^{\phi d}}{C_L^{\phi\phi} + N_L^{\phi,\text{mv}}}\frac{C_L^{\phi d}}{C_L^{dd} + N_L^{d,\text{mv}}}. \tag{44}$$

We set $f_{\text{sky}} = 1$ and sum up tp $L = 100$. We could see that in this ideal case, S/N could reach about 2.5, which still may not be detectable.
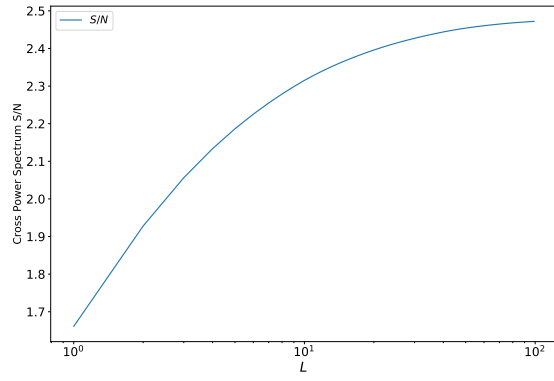
FIG. 5. Cross Power Spectrum S/N Signal to Noise looks really bad for this one...